TUDRP

Modeling of Casing Running in High Angle Wells

Yi Zhang, the University of Tulsa, Drilling Research Projects

This report is prepared for TUDRP Advisory Board Meeting, November 13-14, 2006, Tulsa-Oklahoma.

Abstract

Following the development of Mitchell[1], this report presents a mathematical study of 2-D Soft and Stiff String Torque Analysis with pipe rotation, and a 3-D Soft and Stiff String Drag Analysis with pipe running in and pulling out.

The Torque Analysis has revealed some defects in the conventional formulation. Compared with conventional formulation, for pipe rotation, the term $\sqrt{1+\mu_f^2}$ needs to be included in the contact force calculation.

Comparing the torque calculation equations of 2D Soft and Stiff models, the calculated results are very close.

The change in azimuth results in different doglegs of wellbore, which has great effect on axial force transfer.

Project Status

Tasks	Percentage Accomplished
Literature review	80%
Model development	65%
Results / Data analysis	40%
Reports	40%

Table 1 Project Status

Introduction

During the early years of casing running, the hanging weight of the casing was usually adequate to push it to target depth. Today, more and more extreme long wells are needed to be drilled according to development needs. For example, typical scenarios involve developing offshore reservoirs from nearby shore locations, or using long horizontal

wells to improve oil/gas productivity. Current records for high angle and extended-reach wells exceed 10 km. Due to excessive frictional force between casing string and wellbore, running casing is becoming challenging work[2]. Failure to reach target depth often has a profound consequence on well production and investment benefit[3].

Because of the increased costs and risks in these well, drag and torque analysis is recognized as an important part of the risk management process. Currently, during well planning and drilling operation, two kinds of drag and torque models are mainly used: one is Soft String model developed by Johancsic[4] in 1984; the other is the Stiff String model developed by Ho[5] in 1988. The Soft String model assumes that the string is a weighted cable without stiffness, considering well trajectory curvature but not well trajectory torsion. The Stiff String model by Ho considers the stiffness of drillstrings, but only provides four equilibrium equations, one for moment equilibrium and three for force equilibrium. Some casing gets stuck and fails to achieve the planned depth, even when we are successful in drilling the well. Some problems are a result of inaccurate prediction from existing models, or not understanding the limitations of existing models.

In 2006, Mitchell provided advanced drag and torque analysis (unpublished results) based on constant curvature well trajectories, in which he considers the effect of both wellbore curvature and wellbore torsion.

This report is the second report after my proposal. In my last report, I finished 2-D drag analysis with Soft and Stiff String models. Based on constant curvature method, this report presents the 2-D Soft and Stiff String torque analysis with pipe rotation, and the 3-D Soft and Stiff String drag analysis with pipe running in and pulling out.

General Model with Curvature and Torsionf following the development by Mitchell

The rectangular coordinate system X, Y, Z with the unit vectors $\vec{i}$, $\vec{j}$, $\vec{k}$ and a moving coordinate system with unit vectors $\vec{t}$, $\vec{n}$, $\vec{b}$ are shown in Figure 1.

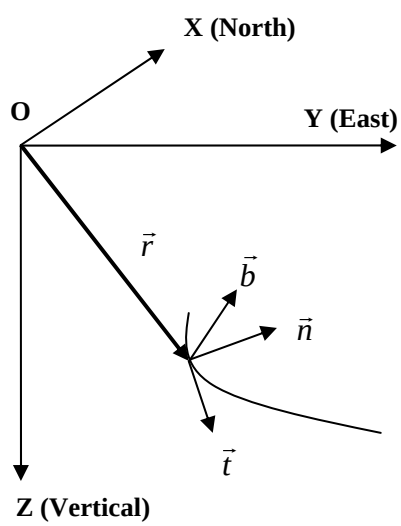

Figure 1: Well coordinate system

The general model for force and moment equilibrium in $\vec{i}$, $\vec{j}$, $\vec{k}$ directions including well curvature and tosiron is as follows[1]:

$$\frac{dF_a}{ds} - F_n\kappa + w_e\vec{k} \bullet \vec{t} + \vec{w}_d \bullet \vec{t} = 0 \tag{1}$$

$$\frac{dF_n}{ds} + F_a\kappa - F_b\tau + w_e\vec{k} \bullet \vec{n} + \vec{w}_c \bullet \vec{n} + \vec{w}_d \bullet \vec{n} = 0 \tag{2}$$

$$\frac{dF_b}{ds} + F_n\tau + w_e\vec{k} \bullet \vec{b} + \vec{w}_c \bullet \vec{b} + \vec{w}_d \bullet \vec{b} = 0 \tag{3}$$

$$\frac{dM_t}{ds} - M_n\kappa + \vec{m} \bullet \vec{t} = 0 \tag{4}$$

$$\frac{dM_n}{ds} + M_t\kappa - M_b\tau - F_b + \vec{m} \bullet \vec{n} = 0 \tag{5}$$

$$\frac{dM_b}{ds} + M_n\tau + F_n + \vec{m} \bullet \vec{b} = 0 \tag{6}$$

where:

κ is well trajectory curvature;

τ is well trajectory torsion.

General Model for Constant Curvature Well Trajectories

Currently, the oil/gas industry is commonly using the constant curvature trajectory method in planning wellbores:

$$\kappa = const. \tag{7}$$

$$\tau = 0 \tag{8}$$

$$\frac{dM_b}{ds} = EI\frac{d\kappa}{ds} = 0 \quad \text{and} \quad M_n = 0 \tag{9}$$

Substituting Equations (7)-(9) into Equations (1)-(6), we get the general Stiff String model for constant curvature well trajectories:

$$\frac{dF_a}{ds} - F_n\kappa + w_e t_z + \vec{w}_d \bullet \vec{t} = 0 \tag{10}$$

$$\frac{dF_n}{ds} + F_a\kappa + w_e n_z + \vec{w}_c \bullet \vec{n} + \vec{w}_d \bullet \vec{n} = 0 \tag{11}$$

$$\frac{dF_b}{ds} + w_e b_z + \vec{w}_c \bullet \vec{b} + \vec{w}_d \bullet \vec{b} = 0 \tag{12}$$

$$\frac{dM_t}{ds} - M_n\kappa + \vec{m} \bullet \vec{t} = 0 \tag{13}$$

$$M_t\kappa - F_b + \vec{m} \bullet \vec{n} = 0 \tag{14}$$

$$F_n + \vec{m} \bullet \vec{b} = 0 \tag{15}$$

where:

$$t_z = \vec{k} \bullet \vec{t} \tag{16}$$

$$n_z = \vec{k} \bullet \vec{n} \tag{17}$$

$$b_z = \vec{k} \bullet \vec{b} \tag{18}$$

Although no stiffness of pipe appears in Equations (10)-(15), the model is applicable to the Stiff String model. It is because of constant curvature well trajectories that the stiffness item will not be shown.

From the above governing equations, it is clear that we need to determine t_z, n_z and b_z in order to calculate drag and torque (see Appendix A).

2-D Soft Model for torque analysis

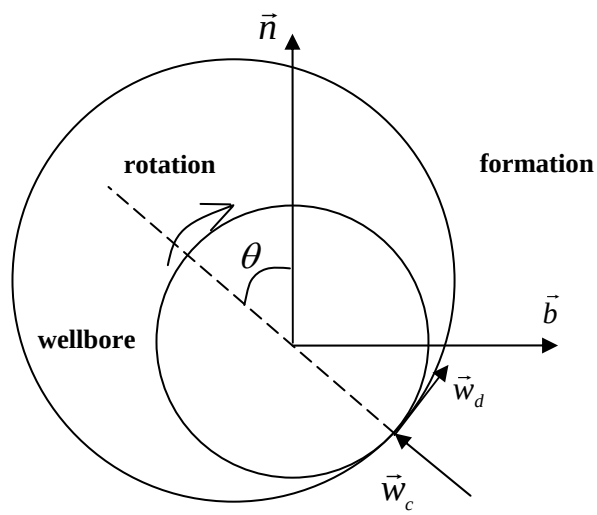

Figure 2: Contact force Angle with rotation

From the general equations for constant curvature well trajectories (Equations (10)-(15)), we have:

$$\frac{dF_a}{ds} + w_e t_z = 0 \tag{19}$$

$$F_a \kappa + w_e n_z + w_c \cos\theta + \mu_f w_c \sin\theta = 0 \tag{20}$$

$$w_e b_z - w_c \sin\theta + \mu_f w_c \cos\theta = 0 \tag{21}$$

$$\frac{dM_t}{ds} - \mu_f w_c r_p = 0 \tag{22}$$

$$M_t \kappa = 0 \tag{23}$$

$$F_n = 0 \tag{24}$$

Equations (20) and (21) yield:

$$w_c(\mu_f \sin\theta + \cos\theta) = -\left(F_a\kappa + w_e n_z\right) \tag{25}$$

$$w_c(\mu_f \cos\theta - \sin\theta) = -w_e b_z \tag{26}$$

From Equations (25) and (26), we get:

$$w_c = \pm\sqrt{\frac{(F_a\kappa + w_e n_z)^2 + (w_e b_z)^2}{1+\mu_f^2}} \tag{27}$$

Rearrange Equations (25) and (26):

$$\frac{\mu_f \cos\theta - \sin\theta}{\mu_f \sin\theta + \cos\theta} = \frac{tg\theta_1 - tg\theta}{1 + tg\theta_1 tg\theta} = tg(\theta_1 - \theta) = \frac{w_e b_z}{(F_a\kappa + w_e n_z)} \tag{28}$$

where: $tg\theta_1 = \mu_f$ (29)

$$\theta = tg^{-1}\mu_f - tg^{-1}\frac{w_e b_z}{(F_a\kappa + w_e n_z)} \tag{30}$$

Assume: $\vec{t}$, $\vec{n}$ are in the same vertical plane, which makes $b_z = 0$. (31)

Substituting Equation (31) into Equation (27) yields:

$$w_c = \frac{\left|F_a\kappa + w_e n_z\right|}{\sqrt{1+\mu_f^2}} \tag{32}$$

$$\theta = tg^{-1}\mu_f \tag{33}$$

The 2-D Torque Analysis by constant curvature method has revealed some defects in the conventional formulation. Comparing with the conventional formulation, for drillstring rotation condition, the term $\sqrt{1+\mu_f^2}$ needs to be included in the contact force calculation: $w_c = \frac{\left|F_a\kappa + w_e n_z\right|}{\sqrt{1+\mu_f^2}}$ (In conventional Soft Model formulation, $w_c = \left|F_a\kappa + w_e n_z\right|$).

According to Equation (19) and the expression of t_z for 2D in Appendix A, we get:

$$F_a(s) = F_a^i + \frac{w_e}{\kappa\sin\beta}\left\{\left\{\cos\left[\kappa\left(s_i - a\right)\right] - \cos\left[\kappa\left(s-a\right)\right]\right\}\cos I_1 + \left[\cos\left(\kappa s\right) - \cos\left(\kappa s_i\right)\right]\cos I_2\right\} \tag{34}$$

where: $F_a^i = F_a\left(s_i\right)$

Combining Equations (22) and (32), we have:

If $F_a\kappa + w_e n_z \geq 0 \quad \Rightarrow$

$$M_t(s) = M(s_i) - \frac{\mu_f r_p}{\sqrt{1+\mu_f^2}} \int_{s_i}^{s} (F_a \kappa + w_e n_z) ds$$

$$= M(s_i) - \frac{\mu_f r_p}{\sqrt{1+\mu_f^2}} \left\{ \left\{ F_a^i \kappa (s - s_i) + \frac{w_e}{\sin\beta} \{\cos[\kappa(s_i - a)]\cos I_1 - \cos(\kappa s_i)\cos I_2\}(s - s_i) \right\} \right.$$

$$+ \frac{w_e}{\kappa \sin\beta} \{[\sin(\kappa s) - \sin(\kappa_i s)]\cos I_2 - \{\sin[\kappa(s-a)] - \sin[\kappa(s_i - a)]\}\cos I_1\}$$

$$\left. + \frac{w_e}{\kappa \sin^2\beta} \sin(I_1 - I_2)\{\{\cos[\kappa(s-a)] - \cos[\kappa(s_i - a)]\}\sin I_1 - [\cos(\kappa s) - \cos(\kappa s_i)]\sin I_2\} \right\} \tag{35}$$

If $F_a \kappa + w_e n_z < 0 \quad \Rightarrow$

$$M_t(s) = M(s_i) + \frac{\mu_f r_p}{\sqrt{1+\mu_f^2}} \int_{s_i}^{s} (F_a \kappa + w_e n_z) ds \tag{36}$$

2-D Stiff Model for torque analysis

Also, from the general equations for constant curvature well trajectories:

$$\frac{dF_a}{ds} - F_n \kappa + w_e t_z = 0 \tag{37}$$

$$\frac{dF_n}{ds} + F_a \kappa + w_e n_z + w_c \cos\theta + \mu_f w_c \sin\theta = 0 \tag{38}$$

$$\frac{dF_b}{ds} + w_e b_z - w_c \sin\theta + \mu_f w_c \cos\theta = 0 \tag{39}$$

$$\frac{dM_t}{ds} - \mu_f w_c r_p = 0 \tag{40}$$

$$M_t \kappa - F_b = 0 \tag{41}$$

$$F_n = 0 \tag{42}$$

Substituting Equation (42) into Equations (37) and (38), and substituting Equation (41) into Equation (39), we have:

$$\frac{dF_a}{ds} + w_e t_z = 0 \tag{43}$$

$$F_a \kappa + w_e n_z + w_c \cos\theta + \mu_f w_c \sin\theta = 0 \tag{44}$$

$$\kappa \mu_f w_c r_p + w_e b_z - w_c \sin\theta + \mu_f w_c \cos\theta = 0 \tag{45}$$

$$\frac{dM_t}{ds} = \mu_f w_c r_p \tag{46}$$

Equations (44) and (45) give:

$$w_c(\mu_f \sin\theta + \cos\theta) = -\left(F_a\kappa + w_e n_z\right) \tag{47}$$

$$w_c(\mu_f \cos\theta - \sin\theta) = -(w_e b_z + \kappa\mu_f w_c r_p) \tag{48}$$

So,

$$\frac{\mu_f \cos\theta - \sin\theta}{\mu_f \sin\theta + \cos\theta} = \frac{tg\theta_1 - tg\theta}{1 + tg\theta_1 tg\theta} = tg(\theta_1 - \theta) = \frac{w_e b_z + \kappa\mu_f w_c r_p}{(F_a\kappa + w_e n_z)} \tag{49}$$

where: $tg\theta_1 = \mu_f$ (50)

$$\theta = tg^{-1}\mu_f - tg^{-1}\frac{w_e b_z + \kappa\mu_f w_c r_p}{(F_a\kappa + w_e n_z)} \tag{51}$$

Also, from Equations (47) and (48), we get:

$$w_c^2[1 + \mu_f^2 + (\kappa\mu_f r_p)^2] + 2w_c w_e b_z \kappa\mu_f r_p - (F_a\kappa + w_e n_z)^2 - w_e^2 b_z^2 = 0 \tag{52}$$

So,

$$w_c = \frac{-w_e b_z \kappa\mu_f r_p \pm \sqrt{(w_e b_z \kappa\mu_f r_p)^2 + [1 + \mu_f^2 + (\kappa\mu_f r_p)^2][(F_a\kappa + w_e n_z)^2 + (w_e b_z)^2]}}{1 + \mu_f^2 + (\kappa\mu_f r_p)^2} \tag{53}$$

If $r_p = 0$, then Equation (53) will be simplified to the same form as the equation (27) for unit contact force in 2-D Soft Model of torque analysis.

Assume: $\vec{t}$, $\vec{n}$ are in the same vertical plane (that also means no change in azimuth of well trajectory), which makes $b_z = 0$.

Equation (51) is simplified into:

$$\theta = tg^{-1}\mu_f - tg^{-1}\frac{\kappa\mu_f w_c r_p}{(F_a\kappa + w_e n_z)} \tag{54}$$

And

$$w_c = \frac{\left|F_a\kappa + w_e n_z\right|}{\sqrt{1 + \mu_f^2 + (\kappa\mu_f r_p)^2}} \tag{55}$$

Similarly, according to Equation (43) and the expression of t_z for 2D in Appendix A, we get:

$$F_a(s) = F_a^i + \frac{w_e}{\kappa\sin\beta}\{\{\cos[\kappa(s_i - a)] - \cos[\kappa(s - a)]\}\cos I_1 + [\cos(\kappa s) - \cos(\kappa s_i)]\cos I_2\} \tag{56}$$

Combining Equations (46) and (55), we have:

If $F_a\kappa + w_e n_z \geq 0 \quad \Rightarrow$

$$M_t(s) = M(s_i) - \frac{\mu_f r_p}{\sqrt{1+\mu_f^2 + (\kappa\mu_f r_p)^2}} \int_{s_i}^{s} (F_a\kappa + w_e n_z) ds$$

$$= M(s_i) - \frac{\mu_f r_p}{\sqrt{1+\mu_f^2 + (\kappa\mu_f r_p)^2}} \left\{ \left\{ F_a^i \kappa (s - s_i) + \frac{w_e}{\sin\beta} \{\cos[\kappa(s_i - a)]\cos I_1 - \cos(\kappa s_i)\cos I_2\}(s - s_i) \right\} \right.$$

$$+ \frac{w_e}{\kappa \sin\beta} \{[\sin(\kappa s) - \sin(\kappa_i s)]\cos I_2 - \{\sin[\kappa(s-a)] - \sin[\kappa(s_i - a)]\}\cos I_1\}$$

$$\left. + \frac{w_e}{\kappa \sin^2\beta} \sin(I_1 - I_2)\{\{\cos[\kappa(s-a)] - \cos[\kappa(s_i - a)]\}\sin I_1 - [\cos(\kappa s) - \cos(\kappa s_i)]\sin I_2\} \right\}$$

(57)

If $F_a\kappa + w_e n_z < 0 \quad \Rightarrow$

$$M_t(s) = M(s_i) + \frac{\mu_f r_p}{\sqrt{1+\mu_f^2 + (\kappa\mu_f r_p)^2}} \int_{s_i}^{s} (F_a\kappa + w_e n_z) ds \tag{58}$$

Comparing the calculation equations for 2-D Soft and Stiff models of torque analysis, we can see that the torque calculation results using Soft and Stiff models are very close:

$$M_t(s) = M(s_i) - \frac{\mu_f r_p}{\sqrt{1+\mu_f^2}} \int_{s_i}^{s} |F_a\kappa + w_e n_z| ds \qquad (Soft\ \ Model)$$

$$M_t(s) = M(s_i) - \frac{\mu_f r_p}{\sqrt{1+\mu_f^2[1+(\kappa r_p)^2]}} \int_{s_i}^{s} |F_a\kappa + w_e n_z| ds \qquad (Stiff\ \ Model)$$

For example, if we take a radius of wellbore R=100ft $(\kappa = 0.01\ ft^{-1})$ and pipe OD=9.625 in $(r_p = 0.4\ ft)$,

$$\Rightarrow \sqrt{1+\mu_f^2[1+(\kappa r_p)^2]} = \sqrt{1+\mu_f^2(1+0.004^2)} = \sqrt{1+\mu_f^2(1.000016)} = \sqrt{1+\mu_f^2}$$

3-D Soft String Model for Drag Analysis

Derivation of Governing Equation for Drag Analysis

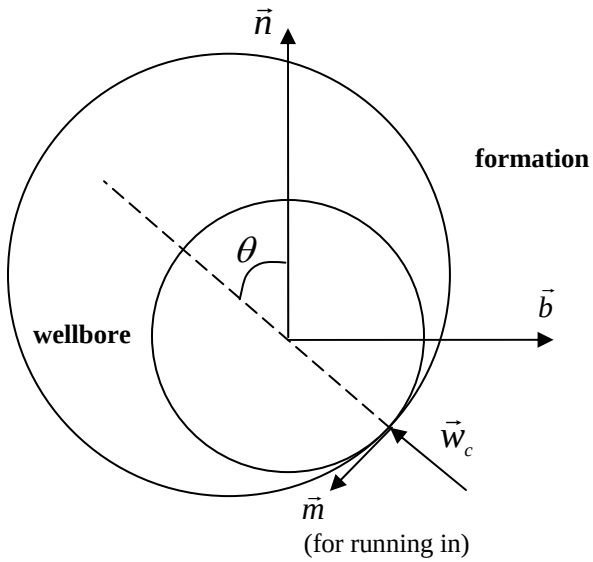

Figure 3: Contact angel with pipe running in and pulling out

Two important assumptions:

(1) Assume that the drag force between pipe and wellbore is linear Coulomb friction. From Figure 3, we get:

$$\vec{w}_d \bullet \vec{t} = \mp w_d = \mp \mu_f |w_c| \text{ (running in for "-"; pulling out for "+")} \quad (59)$$

$$\vec{w}_d \bullet \vec{n} = 0 \quad (60)$$

$$\vec{w}_d \bullet \vec{b} = 0 \quad (61)$$

(2) The shear forces F_n and F_b equal to zero:

$$F_n = 0 \quad (62)$$

$$F_b = 0 \quad (63)$$

Define θ as the contact angle between $\vec{n}$ and $\vec{w}_c$, as shown in Figure 8. We have:

$$\vec{w}_c \bullet \vec{n} = w_c \cos\theta \quad (64)$$

$$\vec{w}_c \bullet \vec{b} = -w_c \sin\theta \quad (65)$$

For force equilibrium without pipe rotation:

$$M_t = 0 \quad (66)$$

Substituting the above equations into Equations(10)-(15) yields Equations (67), (68) and (69). Assume that pipe is being run into the hole. When pipe is being pulled out of the hole, we only need to change $-\mu$ into $+\mu$ in Equation (67).

$$\frac{dF_a}{ds} + w_e t_z - \mu |w_c| = 0 \tag{67}$$

$$F_a \kappa + w_e n_z + w_c \cos\theta = 0 \tag{68}$$

$$w_e b_z - w_c \sin\theta = 0 \tag{69}$$

Equations (68) and (69) yield:

$$w_c^2 = (F_a \kappa + w_e n_z)^2 + (w_e b_z)^2 \tag{70}$$

$$\theta = tg^{-1}\left(\frac{w_e b_z}{-(F_a \kappa + w_e n_z)}\right) \tag{71}$$

Substituting Equation (70) into Equation (67), we get the governing equation (72):

$$\frac{dF_a}{ds} + w_e t_z - \mu_f \sqrt{(F_a \kappa + w_e n_z)^2 + (w_e b_z)^2} = 0 \tag{72}$$

And initial value condition is: $F_a(s = s_i) = F_a^i$

Because the differential equation (72) is complicated, we can not get the analytical solution. A numerical method must be used to solve the problem.

3-D Stiff String Model for Drag Analysis

Derivation of Governing Equation for Drag Analysis

From Figure 2, we know:

$$\vec{w}_c \bullet \vec{n} = w_c \cos\theta \tag{79}$$

$$\vec{w}_c \bullet \vec{b} = -w_c \sin\theta \tag{80}$$

$$\vec{m} \bullet \vec{n} = \mp \mu_f r_p w_c \sin\theta \qquad \text{(running in for “-”; pulling out for “+”)} \tag{81}$$

$$\vec{m} \bullet \vec{b} = \mp \mu_f r_p w_c \cos\theta \qquad \text{(running in for “-”; pulling out for “+”)} \tag{82}$$

For simplification, assume that the pipe is being run into the hole. For the case of pipe being pulled out of hole, we only need to change $-\mu_f$ into $+\mu_f$.

Substituting Equations (79)-(82) into Equations (10)-(15) yields:

$$\frac{dF_a}{ds} - F_n \kappa + w_e t_z - \mu_f |w_c| = 0 \tag{83}$$

$$\frac{dF_n}{ds} + F_a \kappa + w_e n_z + w_c \cos\theta = 0 \tag{84}$$

$$\frac{dF_b}{ds} + w_e b_z - w_c \sin\theta = 0 \tag{85}$$

$$\vec{m} \bullet \vec{t} = 0 \tag{86}$$

$$-F_b - \mu_f r_p w_c \sin\theta = 0 \tag{87}$$

$$F_n - \mu_f r_p w_c \cos\theta = 0 \tag{88}$$

From Equations (87) and (88), we get:

$$w_c \sin\theta = \frac{-F_b}{\mu_f r_p} \tag{89}$$

$$w_c \cos\theta = \frac{F_n}{\mu_f r_p} \tag{90}$$

$$\mu_f \left| w_c \right| = \frac{\sqrt{F_n^2 + F_b^2}}{r_p} \tag{91}$$

$$\theta = tg^{-1}\left(\frac{-F_b}{F_n} \right) \tag{92}$$

Substituting Equations (89), (90) and (91) into Equations (83), (84) and (85), we get the 3-D Stiff String model for drag analysis:

$$\frac{dF_a}{ds} - \kappa F_n + w_e t_z - \frac{\sqrt{F_n^2 + F_b^2}}{r_p} = 0 \tag{93}$$

$$\frac{dF_n}{ds} + \kappa F_a + w_e n_z + \frac{F_n}{\mu_f r_p} = 0 \tag{94}$$

$$\frac{dF_b}{ds} + w_e b_z + \frac{F_b}{\mu_f r_p} = 0 \tag{95}$$

And three initial value conditions:

$$F_a(s = s_i) = F_a^i$$

$$F_n(s = s_i) = F_n^i$$

$$F_b(s = s_i) = F_b^i$$

Case Study

Case 1: Axial force F_a coupled with torque M_t (2D Torque Analysis)

The well trajectory parameters (see Figure 1-Appendix B, which are also same the parameters used in Case 3 of the first ABM report):

KOP=1312 ft,	Casing OD=9 5/8 inch,
Radius of arc section =1910 ft,	Unit weight in air =40 lbf/ft,
Arc length=2332 ft,	Mud density=12.8,
Tangent length=14787 ft,	Friction coefficient =0.4.
Tangent angle=70 degrees,	At bottom: torque=2000 ft-lbf, axial force=0

Table 2: Well parameters for case 1

The effect of frictional coefficient

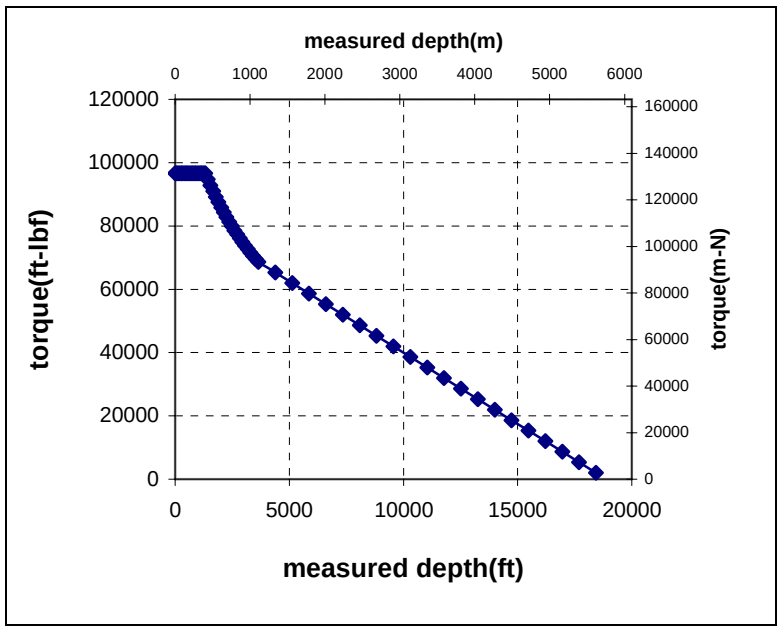

Figure 4

From Figure 4, if we rotate a 9 $^5/_8$-inch casing to the bottom of the wellbore, the surface torque will be very high and reach 97,000 ft-lbf. This will exceed the maximum torque that most of top drive facilities can provide, which means we need to select a larger facility to handle this. The above calculation is based on well quality in which friction coefficient $\mu_f = 0.4$.

If the well quality is improved, the friction coefficient μ_f is reduced, and the surface torque is decreased greatly. Figure 5 shows the different surface torque values when frictional coefficient is 0.4, 0.3, 0.2 and 0.15 respectively.

It's unexpected to find that although changing frictional coefficient changes torque transfer situation, the axial transfer case don't change (see Figure 6). According to

equation $\frac{dF_a}{ds} + w_e t_z = 0$, the axial transfer is only related to the component of effective unit pipe weight along the path of wellbore. From Figure 7, we can see that the change of frictional coefficient does effect the unit contact force, but the difference is small in this case.

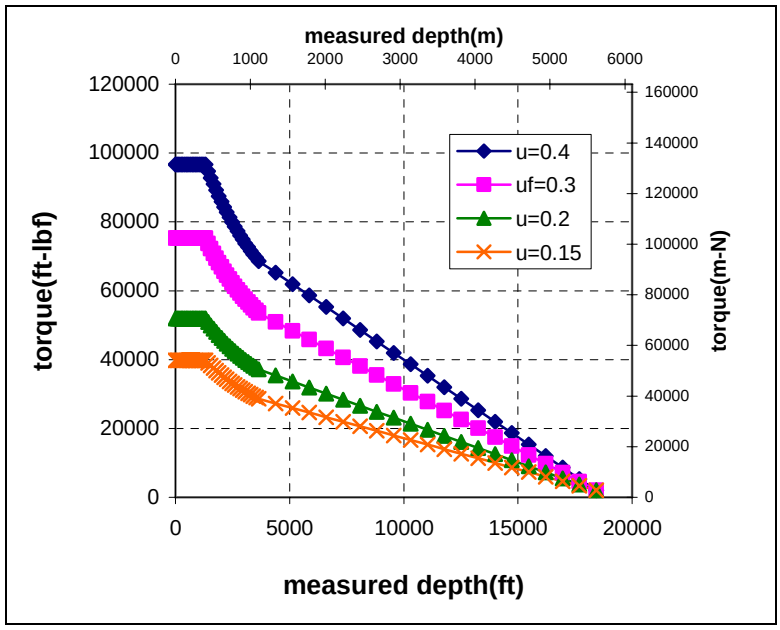

Figure 5

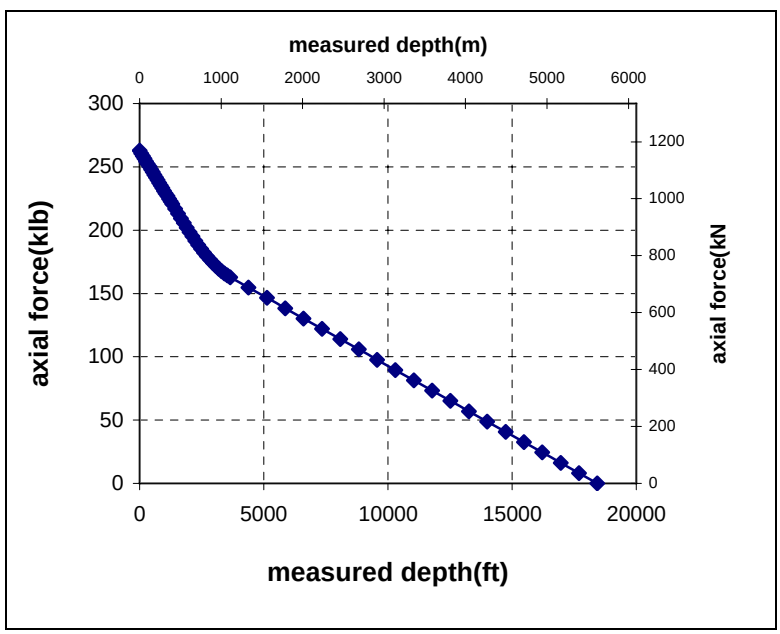

Figure 6

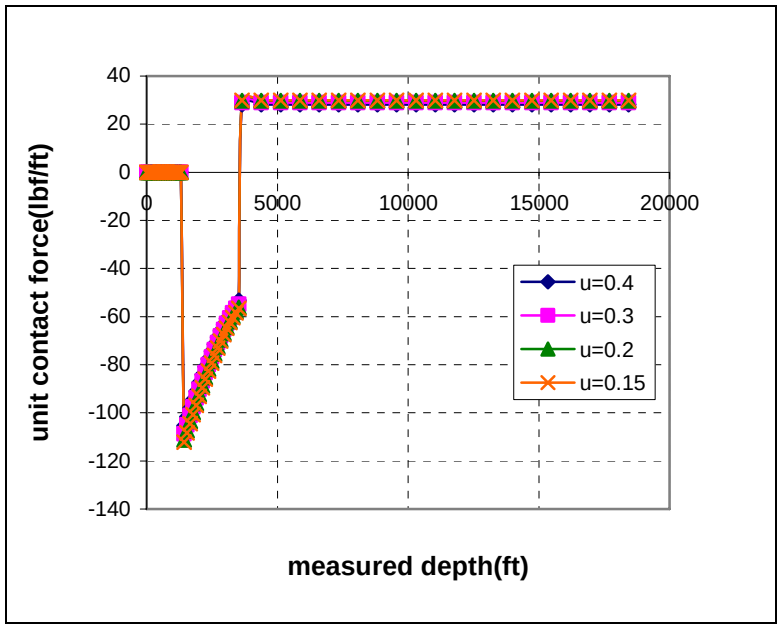

Figure 7

The effect of Pipe OD

Casing Size (in)	Casing weight (lbf/ft)	Casing Grade
9.625	40	J55
7	23	L80
5.5	17	P110
Friction coefficient =0.2		

Table 3

From Figures 5-7, which depict the effect of frictional coefficient for case 1, we can see that with the better well quality (smaller frictional coefficient), the maximum torque needed by the top drive facility is reduced, but the hookload stays at a high value. Figures 8-10 show the effect of pipe OD on torque, axial force and unit contact force when running casing.

From Figure 8, under the condition of frictional coefficient 0.2, the surface torque for 9 $^{5}/_{8}$", 7" and 5.5" casings are 52 kft-lbf, 23 kft-lbf and 14 kft-lbf, respectively. The larger the casing OD, the higher is the surface torque value. This also means that for running larger casing to target depth, the friction between casing and wellbore will require more torque. From Figure 9, we can also see that the larger the casing OD, the larger is the hookload. This means, larger OD casing will require larger "push force" to push casing, or larger weight on bit. From Figure 10, it is clear that larger OD casing has larger unit contact force when pipe is rotating and the torque loss due to the frictional force will be much larger. In addition, the negative values for unit contact forces at arc section means that with high tension force, the casing will touch the upper side of the wellbore.

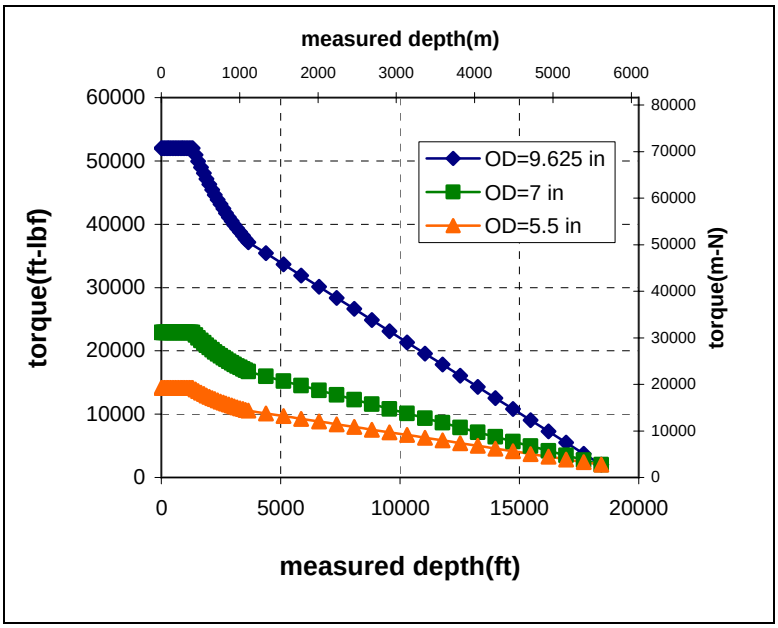

Figure 8

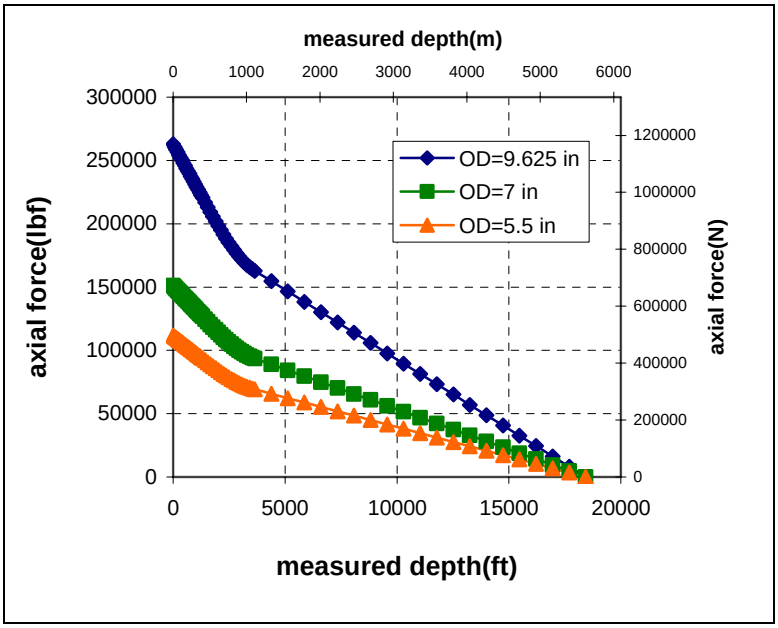

Figure 9

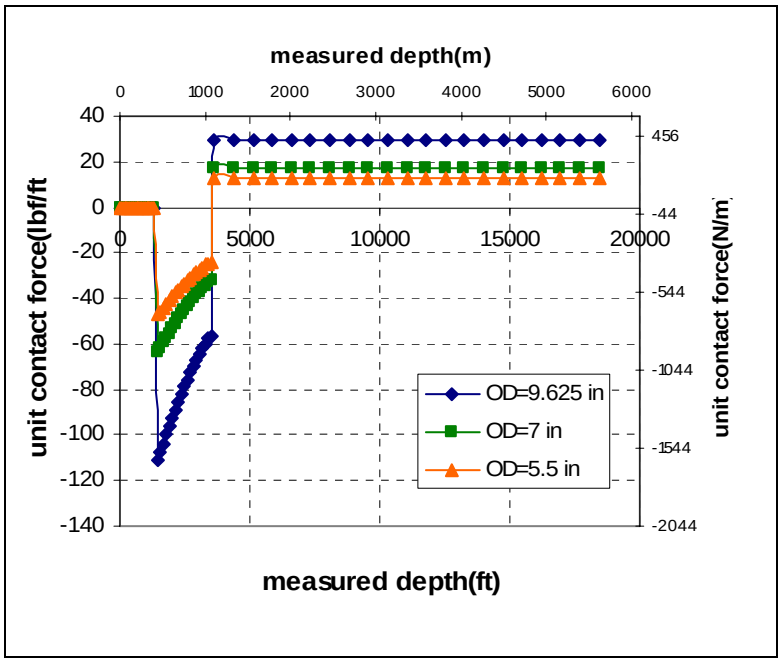

Figure 10

The effect of radius of wellbore

We change a few well parameters of Case 1 in the following to study the effect of radius (see Figure 2-Appendix B), in which the curvature of the arc is 4.7 degrees/100ft, while the original curvature is 3.0 degrees/100ft. The target depth is the same as the original.

KOP=1312 ft,
Radius of arc section =1200 ft,
Arc length=1465 ft,
Tangent length=15460 ft,
Tangent angle=70 degrees,
Friction coefficient=0.3.

Table 4: Parameters for well trajectory with R=1200 ft

From Figure 11, with the same target depth, when we change original radius of curvature from R=1910 ft (curvature=3 degrees/100ft) to R=1200 ft (curvature=4.7 degrees/100ft), the needed surface torque will increase from the original 52 kft-lbf to 55 kft-lbf, about 6% difference. From Figure 12, there is the higher unit contact force in the arc section R=1200 ft than in the arc section R=1910 ft.

It is necessary to point out that although the larger radius of arc will be helpful to torque transfer in this scenario, we will need a longer wellbore. For the scenario of R= 1910 ft, we need to drill a total length of 17120 ft, while for the scenario of R=1200 ft, we only need to drill a total length of 16925 ft.

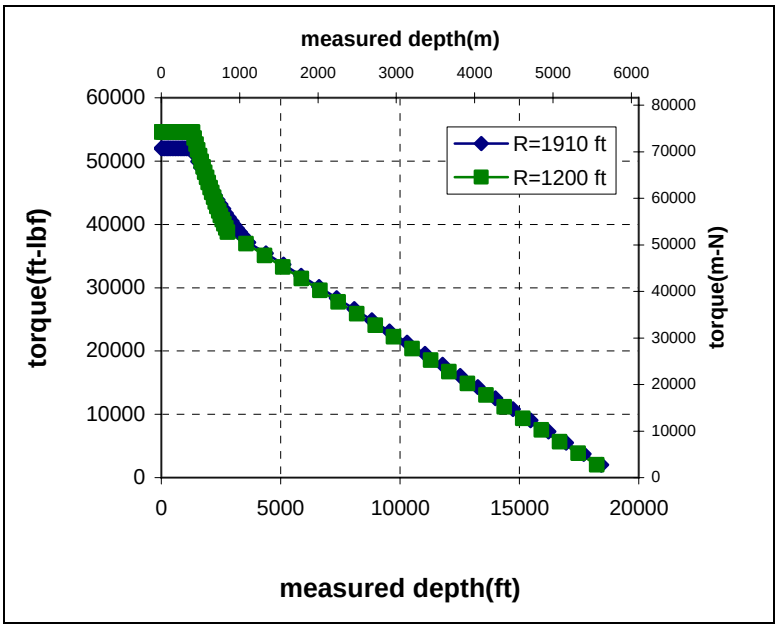

Figure 11

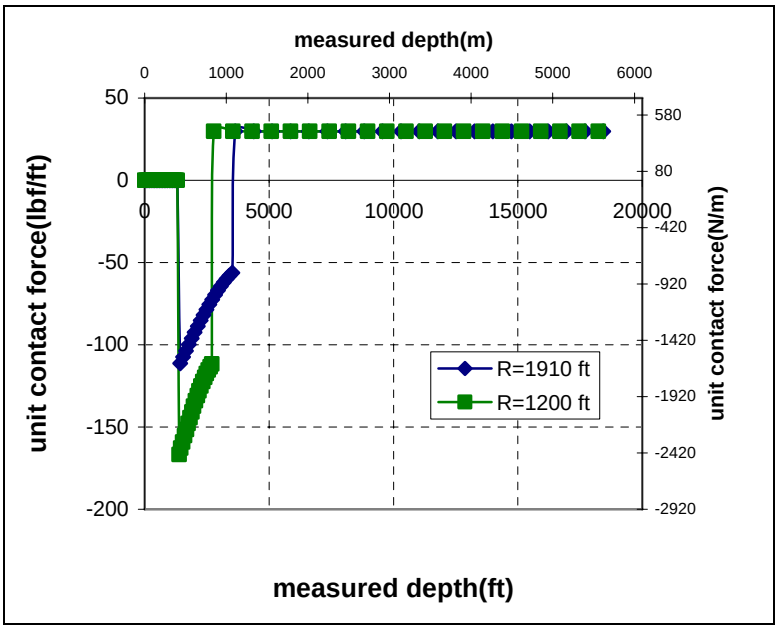

Figure 12

Case 2: Comparison of 2-D and 3-D Soft Drag Models-the effect of azimuth

At survey stations 1 and 2, the measured data is as follows (also see Figure 3-Appendix B):

Point 1	I_1 =13.4 degrees	A_1 =255 degrees (S75W)
Point 2	I_2 =16.3 degrees	A_2 =255 degrees (S75W)
Dogleg=2.9 degrees/100ft		
The length between point 1 and point 2: Δs =100 ft		
Axial force at pipe bottom F_2 =30,000 lbf	Effective pipe weight w_e =15 lbf/ft	
Friction coefficient μ_f =0.3		

Table 5

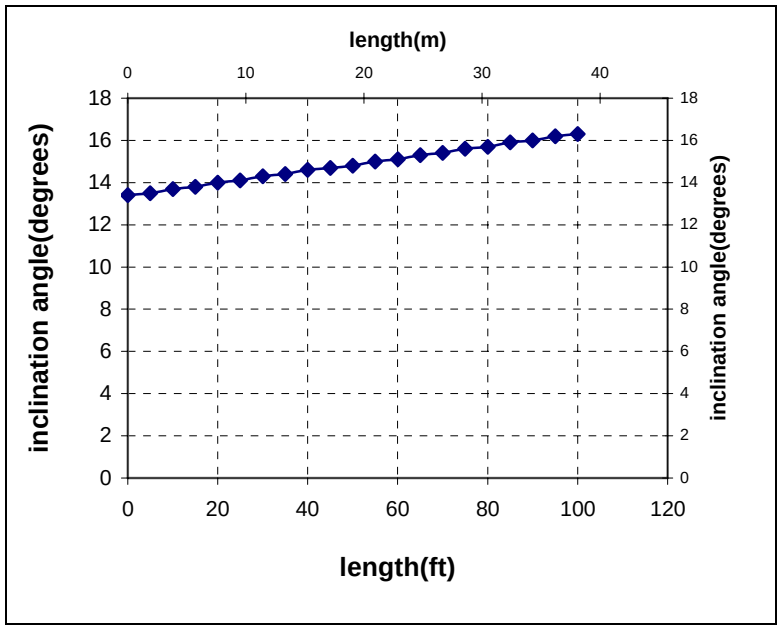

Figure 13

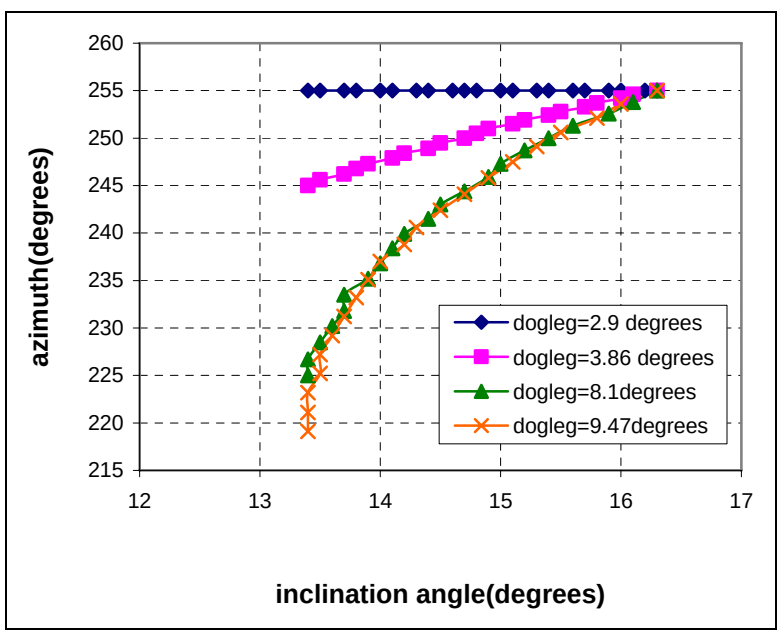

Figure 14

In Figure 15, although the design well trajectory (two dimensional) has a good result for axial force transfer (dogleg=2.9degrees/100ft), in real drilling if azimuth changes from A_1=219 degrees to A_2=255 degrees (dogleg=9.47 degrees/100ft), the pipe will be "locked" and the weight of upper casing can not effectively transfer. From Figure 16, it is clear that the higher the dogleg is, the higher the unit contact force will be.

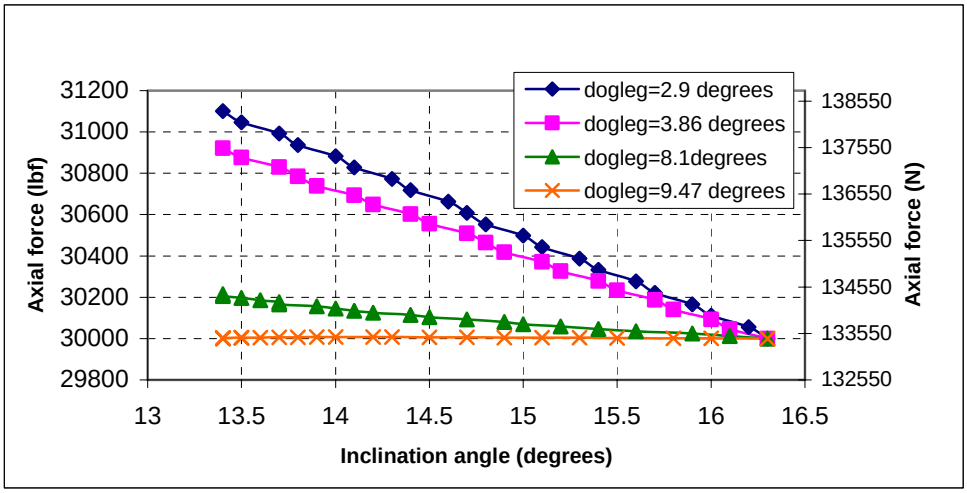

Figure 15: The effect of Azimuth on axial force transfer

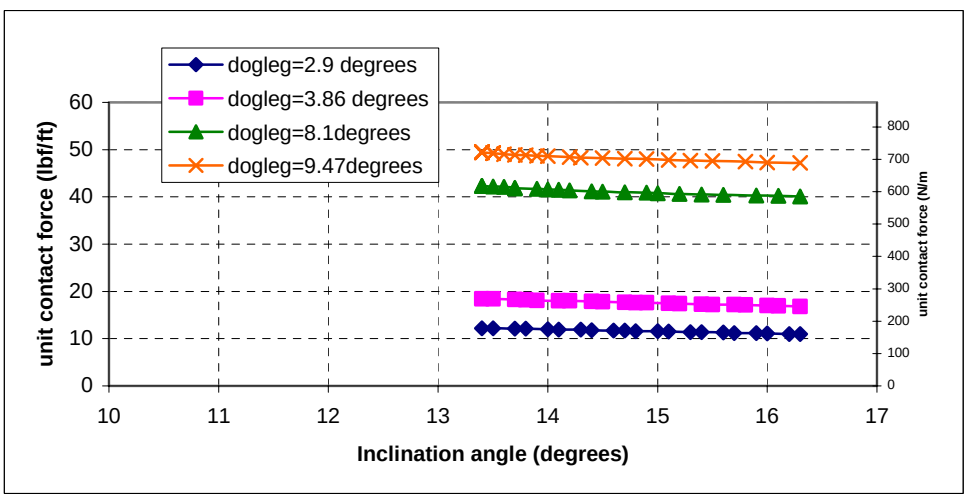

Figure 16: The effect of Azimuth on axial unit contact force

Closing Remarks

1. The 2-D Torque Analysis by constant curvature method has revealed some defects in the conventional formulation. Comparing with conventional formulation, for drillstring rotation condition, the term $\sqrt{1+\mu_f^2}$ needs to be included in the contact force calculation: $w_c = \dfrac{|F_a\kappa + w_e n_z|}{\sqrt{1+\mu_f^2}}$ (Conventional Soft Model formulation, $w_c = |F_a\kappa + w_e n_z|$).

2. Comparing the calculation equations for 2-D soft and stiff models of torque analysis, the torque calculation results using soft and stiff models are very close.

3. Frictional coefficient has very important effect on torque transfer.

4. When casing is rotating, larger OD casing produces larger “pushing force” to run casing, but the higher contact force causes the higher torque loss.

5. The change in azimuth of wellbore results in different doglegs of wellbore, which has great effect on axial force transfer.

Future Work

1. Develop 3-D Soft and Stiff String Models with rotation.
2. Case Study for 3-D Soft and Stiff String Models using field data.
3. Try to consider torsion in the 3-D Soft and Stiff String Models.

Nomenclature

I = inclination angle at an arbitrary point of well trajectory, radians
A = azimuth at an arbitrary point of well trajectory, radians
κ = wellbore curvature, 1/ft
τ = well trajectory torsion, 1/ft
β = dogleg between point 1 and point 2, radians
a = the total arc length between point 1 and point 2
s = the arc length between point 1 and point M, ft
$\vec{m}$ = unit moment caused by friction
$\vec{i}$ = unit vector of X direction
$\vec{j}$ = unit vector of Y direction
$\vec{k}$ = unit vector of Z direction
$\vec{t}$ = unit vector in tangent direction of pipe
$\vec{n}$ = unit vector in normal direction of pipe
$\vec{b}$ = unit vector in binormal direction of pipe
F_a = axial force, lbf
F_n = shear force in normal direction, lbf
F_b = shear force in binormal direction, lbf
w_e = buoyant weight of pipe per unit length, lbf/ft
w_c = unit contact force, lbf/ft
w_d = friction force per unit length, lbf/ft
M_t = moment in tangent direction, ft-lbf
M_n = moment in normal direction, ft-lbf
M_b = moment in binormal direction, ft-lbf
I_1 = inclination angle at point 1, radians
I_2 = inclination angle at point 2, radians
A_1 = azimuth at point 1, radians

A_2 = azimuth at point 2, radians

μ_f = friction coefficient

F_a^i = initial axial force at $s = s_i$, lbf

F_a^{i+1} = initial axial force at $s = s_{i+1}$, lbf

References

1. Mitchell, Robert F., "Advanced Torque-Drag Analysis", 2006.
2. Colin J. Mason, Jesse Lopez, Sigve Meling, Robert Munger, "Casing Running Challengers for Extended-Reach Wells", the SPE Annual Technical Conference and Exhibition held in Denver, Colorado, 5-8 October 2003.
3. C.J.Mason, D.C.-K. Chen, "The Drilling and Casing Running Enigma", the 2006 SPE Annual Technical Conference and Exhibition, San Antonio, Texas, 24-27 September 2006.
4. C. A. Johancsik, D.B. Friesen, Rapier Dawson, "Torque and Drag in Directional Wells-Prediction and Measurement", SPE 11380, IADC/SPE Conference, New Orleans, 1993.
5. H-S. Ho, "An Improved Modeling Program for Computing the Torque and Drag in Directional and Deep Wells", the 63rd Annual Technical Conference and Exhibition of SPE, Houston, Texas, October 2-5, 1988.
6. D. A. Cocking, P.N. Bezant, P.J. Toms, "Pushing the ERD Envelope at Wytch Farm", SPE/IADC 37618, the 1997 SPE/IADC Drilling Conference, Amsterdam, The Netherlands, 4-6 March 1997.
7. Viktorin, R.A., McDermott, J.R., Rush Jr., R.E., and Schamp, J.H., "The Next Generation of Sakhalin Extended-Reach Drilling", IADC/SPE 99131, IADC/SPE Drilling Conference, Miami, Florida, USA, 21-23 February 2006.
8. Mason, C.J. and Chen, D. C-K., "The Wellbore Quality Scorecard (WQS)", IADC/SPE 98893, IADC/SPE Drilling Conference, Miami, Florida, USA, 21-23 February 2006.
9. R.Rezvani, and B. Techentien, "Torque and Drag Modelling for Horizontal Openhole Completions", the 2005 SPE Annual Technical Conference and Exhibition, Dallas, Texas, 9-12 October 2005.
10. Rezmer-Cooper, I., Chau, M., Hendricks, A., Woodfine, M., Stacey, B. and Downton, N., "Field Data Supports the Use of Stiffness and Tortuosity in Solving Complex Well Design Problems", SPE/IADC 52819, SPE/IADC Drilling Conference, Amsterdam, Netherlands, 9-11 March 1999.
11. Maidla, Eric E., Wojtanowicz, Andrew K., " Prediction of Casing Running Loads in Directional Wells", the 20th Annual OTC in Houston, Texal, May 2-5,1998.
12. Tom Gaynor, Doug Hamer, David C-K Chen, Darren Stuart, "Quantifying Tortuosities by Friction Factors in Torque and Drag Model", the SPE Annual Technical Conference and Exhibition, San Antonio, Texas, 29 September-2 October 2002.
13. Eric Maidla, Marc Haci, "Understanding Torque: The Key to Slide-Drilling Directional Wells", the IADC/SPE Drilling Conference, Dallas, Texas, 2-4 March 2004.

Appendix A:

Determination of t_z, n_z and b_z

1. Minimum Curvature Method

Constant curvature wellbore trajectories are commonly described using the minimum curvature method. In this method, unit binormal vector $\vec{b}$ and curvature κ are constant, and torsion τ is zero, which greatly simplifies the equations.

For the survey data of two adjacent survey points (measured depth, inclination angles I_1 and I_2, azimuth A_1 and A_2), the unit tangent vectors $\vec{t}_1$ and $\vec{t}_2$ at the arc's start and end points can be calculated by Equation (A-1) and Equation (A-2), respectively.

$$\vec{t}_1 = \vec{i}\left(\sin I_1 \cos A_1\right) + \vec{j}\left(\sin I_1 \sin A_1\right) + \vec{k}\left(\cos I_1\right) \tag{A-1}$$

$$\vec{t}_2 = \vec{i}\left(\sin I_2 \cos A_2\right) + \vec{j}\left(\sin I_2 \sin A_2\right) + \vec{k}\left(\cos I_2\right) \tag{A-2}$$

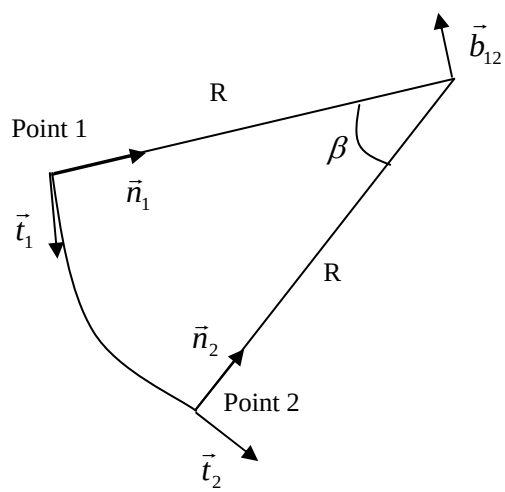

Figure 1: Well geometry of the minimum curvature between two adjacent survey points

The angle between the unit tangent vectors $\vec{t}_1$ and $\vec{t}_2$ is β (dog-leg). We can derive the expression of unit binormal vector $\vec{b}_{12}$ from Equations (A-1) and (A-2).

$$\vec{b}_{12} = \frac{\vec{t}_1 \times \vec{t}_2}{\sin\beta} = \frac{1}{\sin\beta}\Big[\vec{i}\left(\sin I_1 \cos I_2 \sin A_1 - \cos I_1 \sin I_2 \sin A_2\right) - \vec{j}\left(\sin I_1 \cos I_2 \cos A_1 - \cos I_1 \sin I_2 \cos A_2\right)$$
$$+ \vec{k}\left(\sin I_1 \sin I_2 \cos A_1 \sin A_2 - \sin I_1 \sin I_2 \sin A_1 \cos A_2\right)\Big]$$
$$= \frac{1}{\sin\beta}\Big\{\vec{i}\left(\sin I_1 \cos I_2 \sin A_1 - \cos I_1 \sin I_2 \sin A_2\right) - \vec{j}\left(\sin I_1 \cos I_2 \cos A_1 - \cos I_1 \sin I_2 \cos A_2\right)$$
$$+ \vec{k}\left[\sin I_1 \sin I_2 \sin\left(A_2 - A_1\right)\right]\Big\} \tag{A-3}$$

For the whole circular arc between point 1 and point 2, $\vec{b}$ is constant because inclination angles I_1, I_2 and azimuths A_1 and A_2 are known according to survey data.

From the above equations, we can get the expressions of $\vec{n}_1$ and $\vec{n}_2$ at point 1 and point 2:

$$\vec{n}_1 = \vec{b}_{12} \times \vec{t}_1 \tag{A-4}$$

$$\vec{n}_2 = \vec{b}_{12} \times \vec{t}_2 \tag{A-5}$$

2. Determination of t_z, n_z and b_z at any position M on a circular arc

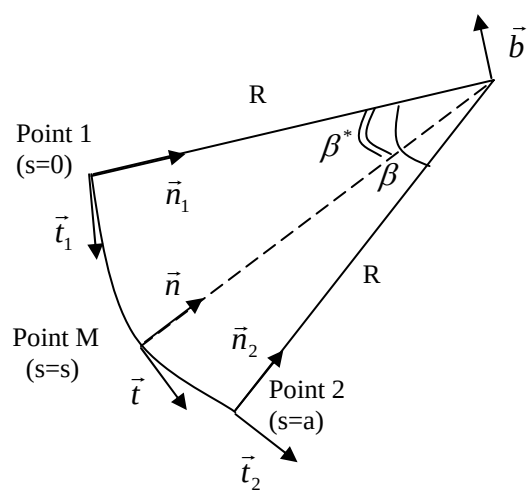

Figure 2: Interpolation at a point on a circular arc

Consider an arbitrary point M at any position on a circular arc (see Figure 2).The unit tangent vector $\vec{t}$ at point M is:

$$\vec{t} = \vec{i}\left(\sin I \cos A\right) + \vec{j}\left(\sin I \sin A\right) + \vec{k}\left(\cos I\right) \tag{A-6}$$

The unit binormal vector can be expressed as:

$$\vec{b} = \frac{\vec{t}_1 \times \vec{t}}{\sin\beta^*} = \frac{\vec{t}_1 \times \vec{t}_2}{\sin\beta} \tag{A-7}$$

where: β^* is the dogleg between unit tangent vectors $\vec{t}_1$ and $\vec{t}$.

Taking the cross product of both sides of the equation (A-7) with $\vec{t}_1$:

$$\frac{\vec{t}_1 \times (\vec{t}_1 \times \vec{t})}{\sin\beta^*} = \frac{\vec{t}_1 \times (\vec{t}_1 \times \vec{t}_2)}{\sin\beta}$$

$$\Rightarrow \frac{(\vec{t}_1 \bullet \vec{t})\vec{t}_1 - (\vec{t}_1 \bullet \vec{t}_1)\vec{t}}{\sin\beta^*} = \frac{(\vec{t}_1 \bullet \vec{t}_2)\vec{t}_1 - (\vec{t}_1 \bullet \vec{t}_1)\vec{t}_2}{\sin\beta}$$

$$\Rightarrow \frac{(\vec{t}_1 \bullet \vec{t})\vec{t}_1 - \vec{t}}{\sin\beta^*} = \frac{(\vec{t}_1 \bullet \vec{t}_2)\vec{t}_1 - \vec{t}_2}{\sin\beta}$$

$$\Rightarrow \vec{t} = (\vec{t}_1 \bullet \vec{t})\vec{t}_1 - \frac{\sin\beta^*}{\sin\beta}\left[(\vec{t}_1 \bullet \vec{t}_2)\vec{t}_1 - \vec{t}_2\right]$$

So,

$$\vec{t} = \vec{t}_1 \cos\beta^* - \frac{\sin\beta^*}{\sin\beta}(\vec{t}_1 \cos\beta - \vec{t}_2) \tag{A-8}$$

Multiply the numerator and denominator of the first term in Equation (A-8) by $\sin\beta$ and collect terms in $\vec{t}_1$ and $\vec{t}_2$:

$$\begin{aligned}\vec{t} &= \vec{t}_1 \cos\beta^* \frac{\sin\beta}{\sin\beta} - \frac{\sin\beta^*}{\sin\beta}(\vec{t}_1 \cos\beta - \vec{t}_2) \\ &= \vec{t}_1 \frac{\sin(\beta - \beta^*)}{\sin\beta} + \vec{t}_2 \frac{\sin\beta^*}{\sin\beta}\end{aligned} \tag{A-9}$$

Substituting Equations (A-1) and (A-2) into Equation (A-9):

$$\begin{aligned}\vec{t} &= \frac{\sin(\beta - \beta^*)}{\sin\beta}\left[\vec{i}(\sin I_1 \cos A_1) + \vec{j}(\sin I_1 \sin A_1) + \vec{k}(\cos I_1)\right] \\ &\quad + \frac{\sin\beta^*}{\sin\beta}\left[\vec{i}(\sin I_2 \cos A_2) + \vec{j}(\sin I_2 \sin A_2) + \vec{k}(\cos I_2)\right] \\ &= \vec{i}\left[\frac{\sin(\beta - \beta^*)\sin I_1 \cos A_1 + \sin\beta^* \sin I_2 \cos A_2}{\sin\beta}\right] + \vec{j}\left[\frac{\sin(\beta - \beta^*)\sin I_1 \sin A_1 + \sin\beta^* \sin I_2 \sin A_2}{\sin\beta}\right] \\ &\quad + \vec{k}\left[\frac{\sin(\beta - \beta^*)\cos I_1 + \sin\beta^* \cos I_2}{\sin\beta}\right]\end{aligned} \tag{A-10}$$

Because the radius of the arc is fixed, and the unit vectors $\vec{t}_1$, $\vec{t}_2$ and $\vec{t}$ are in the same spatial plane, we get:

$$\frac{s}{\beta^*} = \frac{a}{\beta} \tag{A-11}$$

where: a is the length of arc between point 1 and point 2;
s is the length of arc between point 1 and point M.

Combining Equations (A-10) and (A-11) gives:

$$\vec{t} = \vec{i}\,\frac{1}{\sin\beta}\left\{\sin\left[\left(1-\frac{s}{a}\right)\beta\right]\sin I_1\cos A_1 + \sin\left(\frac{s}{a}\beta\right)\sin I_2\cos A_2\right\} + \vec{j}\,\frac{1}{\sin\beta}\left\{\sin\left[\left(1-\frac{s}{a}\right)\beta\right]\sin I_1\sin A_1 + \sin\left(\frac{s}{a}\beta\right)\sin I_2\sin A_2\right\} + \vec{k}\,\frac{1}{\sin\beta}\left\{\sin\left[\left(1-\frac{s}{a}\right)\beta\right]\cos I_1 + \sin\left(\frac{s}{a}\beta\right)\cos I_2\right\} \tag{A-12}$$

Based on Equation (A-7), we can see that $\vec{b}$ is constant for the whole circular arc between point 1 and point 2.

$$\begin{aligned}\vec{b} &= \vec{b}_{12} \\ &= \frac{1}{\sin\beta}\left\{\vec{i}\left(\sin I_1\cos I_2\sin A_1 - \cos I_1\sin I_2\sin A_2\right) + \vec{j}\left(\cos I_1\sin I_2\cos A_2 - \sin I_1\cos I_2\cos A_1\right) + \vec{k}\left[\sin I_1\sin I_2\sin\left(A_2 - A_1\right)\right]\right\}\end{aligned} \tag{A-13}$$

According to Serret-Frenet equations, we get:

$$\begin{aligned}\vec{n} &= \vec{b}\times\vec{t} \\ &= \vec{i}\,\frac{1}{\sin^2\beta}\left\{(\cos I_1\sin I_2\cos A_2 - \sin I_1\cos I_2\cos A_1)\left[\sin(1-\frac{s}{a})\beta\cos I_1 + \sin(\frac{s}{a}\beta)\cos I_2\right] - \left[\sin(1-\frac{s}{a})\beta\sin I_1\sin A_1 + \sin(\frac{s}{a}\beta)\sin I_2\sin A_2\right]\sin I_1\sin I_2\sin(A_2 - A_1)\right\} \\ &+ \vec{j}\,\frac{1}{\sin^2\beta}\left\{\sin I_1\sin I_2\sin(A_2 - A_1)\left[\sin(1-\frac{s}{a})\beta\sin I_1\cos A_1 + \sin(\frac{s}{a}\beta)\sin I_2\cos A_2\right] - (\sin I_1\cos I_2\sin A_1 - \cos I_1\sin I_2\sin A_2)\left[\sin(1-\frac{s}{a})\beta\cos I_1 + \sin(\frac{s}{a}\beta)\cos I_2\right]\right\} \\ &+ \vec{k}\,\frac{1}{\sin^2\beta}\left\{(\sin I_1\cos I_2\sin A_1 - \cos I_1\sin I_2\sin A_2)\left[\sin(1-\frac{s}{a})\beta\sin I_1\sin A_1 + \sin(\frac{s}{a}\beta)\sin I_2\sin A_2\right] + (\sin I_1\cos I_2\cos A_1 - \cos I_1\sin I_2\cos A_2)[\sin(1-\frac{s}{a})\beta\sin I_1\cos A_1 + \sin(\frac{s}{a}\beta)\sin I_2\cos A_2]\right\}\end{aligned} \tag{A-14}$$

t_z, n_z *and* b_z *for 3-D well trajectory*

From Equations (A-12)-(A-14), we get:

$$t_z = \frac{1}{\sin\beta}\left\{\sin\left[\left(1-\frac{s}{a}\right)\beta\right]\cos I_1 + \sin\left(\frac{s}{a}\beta\right)\cos I_2\right\} \tag{A-15}$$

$$n_z = \frac{1}{\sin^2\beta}\left\{(\sin I_1 \cos I_2 \sin A_1 - \cos I_1 \sin I_2 \sin A_2)\left[\sin(1-\frac{s}{a})\beta \sin I_1 \sin A_1 + \sin(\frac{s}{a}\beta)\sin I_2 \sin A_2\right]\right.$$
$$\left. + (\sin I_1 \cos I_2 \cos A_1 - \cos I_1 \sin I_2 \cos A_2)\left[\sin(1-\frac{s}{a})\beta \sin I_1 \cos A_1 + \sin(\frac{s}{a}\beta)\sin I_2 \cos A_2\right]\right\} \quad \text{(A-16)}$$

$$b_z = \left[\sin I_1 \sin I_2 \sin\left(A_2 - A_1\right)\right] \quad \text{(A-17)}$$

For example, if $A_1 = A_2$, t_z, n_z and b_z for 2-D well trajectory

$$t_z = \frac{1}{\sin\beta}\left\{\sin\left[\left(1-\frac{s}{a}\right)\beta\right]\cos I_1 + \sin\left(\frac{s}{a}\beta\right)\cos I_2\right\} = \frac{\sin\left[\kappa\left(a-s\right)\right]\cos I_1 + \sin\left(\kappa s\right)\cos I_2}{\sin\beta} \quad \text{(A-18)}$$

$$n_z = \frac{\sin\left(I_1 - I_2\right)\left\{\sin\left[(1-\frac{s}{a})\beta\right]\sin I_1 + \sin(\frac{s}{a}\beta)\sin I_2\right\}}{\sin^2\beta} = \frac{\sin\left(I_1 - I_2\right)\left\{\sin\left[\kappa\left(a-s\right)\right]\sin I_1 + \sin\left(\kappa s\right)\sin I_2\right\}}{\sin^2\beta} \quad \text{(A-19)}$$

$$b_z = 0 \quad \text{(A-20)}$$

Appendix B:

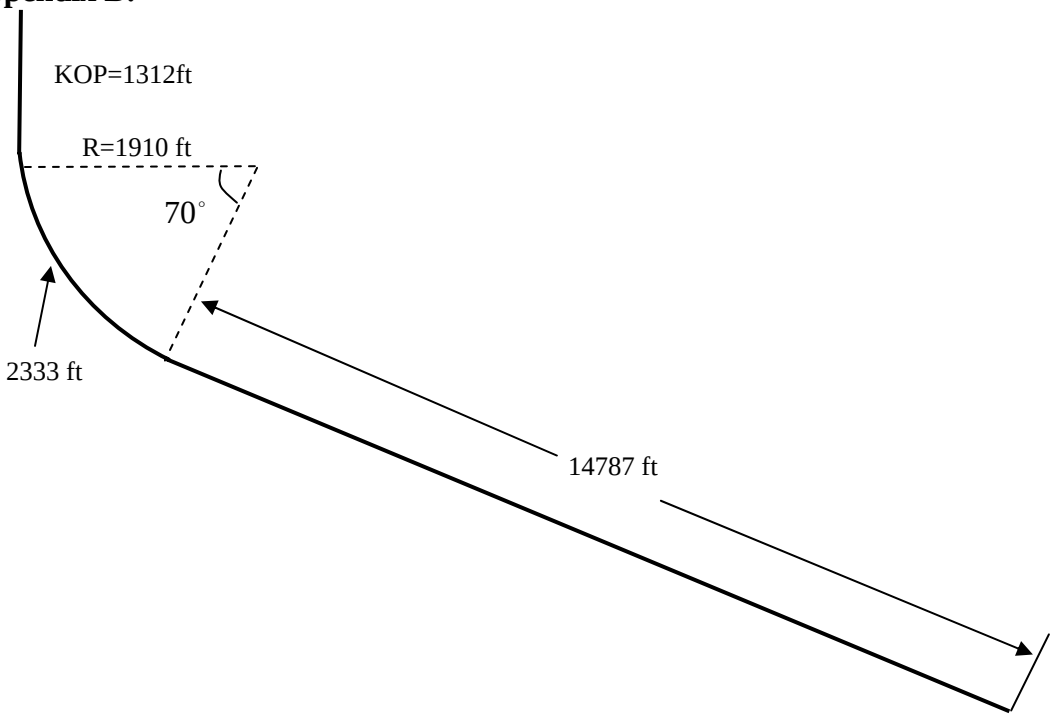

Figure1: The well trajectory-Chirag A16 T2 of British Petroleum Company (casing size=9.625”, unit weight=40 lbf/ft, mud density=12.8, friction coefficient=0.4)

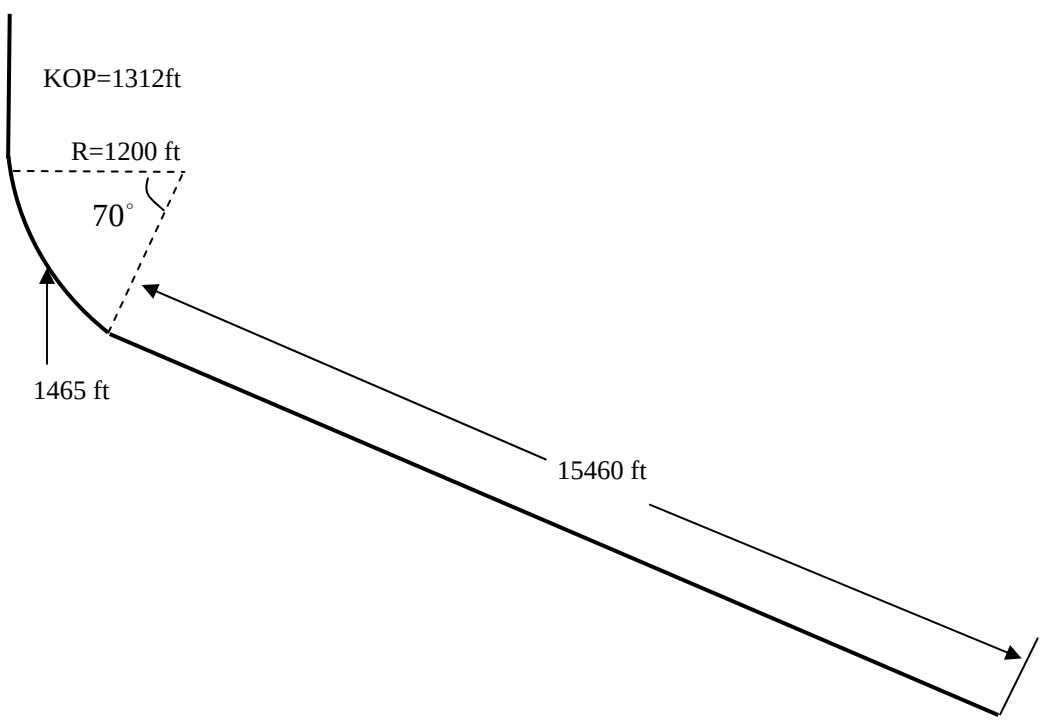

Figure 2: The well trajectory (R=1200 ft) with the same target depth as Figure 1

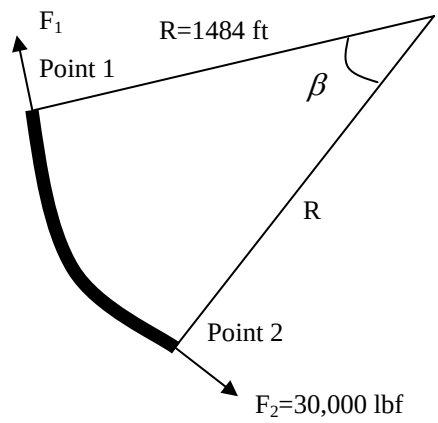

Figure 3 : Well geometry of the minimum curvature between two adjacent survey points